Available online at www.sciencedirect.com
SCIENCE DIRECT®
Carbon 42 (2004) 1665–1670
CARBON
www.elsevier.com/locate/carbon

Fatigue of C/C composites in bending and in shear modes

Yasuhiro Tanabe [a,*], Takuya Yoshimura [a], Tomoyuki Watanabe [a], Toshiharu Hiraoka [b], Yasuhisa Ogita [b], Eiichi Yasuda [a]

[a] Materials and Structures Laboratory, Tokyo Institute of Technology, 4259, Nagatsuta, Midori, Yokohama 226-8503, Japan
[b] Department of Composite Materials, Toyo Tanso Co., Ltd., 2181-2, Nakahime, Ohnohara-cho, Mitoyo-gun 796-1612, Japan

Received 21 August 2003; accepted 17 February 2004
Available online 24 March 2004

Abstract

The fatigue of C/C composites was investigated in bending and shear modes. In bending, a large stress ratio resulted in a decrease in strength; the decrease became small without water present. However, a large ratio led to a decrease in Young's modulus, regardless of the presence of water. In shear, degradation in strength or fatigue life decreased with increasing the ratio. For specimens fatigue degraded in air, static strength in water decreased as compared with that in air. It is strongly suggested that fatigue degradation in C/C composites is promoted by a combination of stress corrosion and crack propagation promoted by a wedge effect.

Keywords: A. Carbon composites; D. Fracture; Mechanical properties

1. Introduction

For the utilization of carbon fiber reinforced carbon matrix composites (C/C composites) in space, new-energy production industries and engineering applications requiring materials with high specific strength above 1200 °C, fatigue behavior is important and obtaining their fatigue data is essential. However, only a few reports have been published on the behavior [1–9], and mainly along the fiber/reinforced direction. In a laminated C/C composite with tensile fatigue loading, a peculiar result that no degradation took place over 10^4 fatigue cycles, even applying ca. 90% of the tensile strength, was obtained; degradation of interfacial bonding seemed to affect the result [9].

Crack propagation during the fatigue tests of polycrystalline graphites seems to correlate to a type of cleavage in crystallites/grains [10,11]. It is also reported that adsorbed water affected their strength [12]. However, even in polycrystalline graphites, enough data are not available for elucidating the fatigue mechanism and on factors affecting their fatigue mechanisms/behavior.

In C/C composites, static strength was decreased by adsorbed water [13], but details were not investigated. No clear reports have been presented to date dealing with the effects of water on fatigue degradation/properties in C/C composites. The effects seem to be different in bending and shear modes, because the properties of the former are dominated by reinforcing fibers and the latter by the matrix. Comprehensive studies are necessary.

Therefore, in this study, fatigue tests were carried out in the bending and shear modes using the same C/C composites to obtain comprehensive data on the fatigue fracture of the composites. Effects of water on the tested composites were also investigated.

2. Experimental

2.1. Fatigue in the bending mode

2.1.1. Materials

Two types of laid-up C/C composites, finally heat treated at 2000 °C, were used in this mode: C6-Pi3 and C6-Pi3-V. Both were reinforced with a two-dimensional plain-woven fabric, denoted as C6, consisting of tows having 6000 filaments of PAN-based fiber (strength: 3.53 GPa, Young's modulus 230 GPa), and had a three-time

* Corresponding author. Tel.: +81-45-924-5356; fax: +81-45-924-5345.
E-mail address: y.tanabe@msl.titech.ac.jp (Y. Tanabe).

0008-6223/$ - see front matter © 2004 Elsevier Ltd. All rights reserved.
doi:10.1016/j.carbon.2004.02.022

Table 1
Characteristics of the C/C composites used in this study

Sample	Volume fraction of fiber in vol%	Open porosity in %	Apparent density in Mg/m^3	Bending strength in MPa	Inter laminar shear strength (ILSS) in MPa
C6-Pi1	55.3	12.1	1.52	114	5.8
C6-Pi3	55.4	8.1	1.65	236	9.8
C6-Pi3-V	53.0	9.1	1.59	168	6.3
CN6-Pi3	56.8	9.1	1.56	136	7.4
C6-Ph3	55.1	8.0	1.58	190	8.2
CN6-Ph3	56.5	9.4	1.54	134	6.6
SY-Pi1	53.1	14.9	1.36	51	4.1
SY-Pi4	53.6	7.2	1.58	115	12.7
SY-Ph1	53.5	17.0	1.37	64	7.1
SY-Ph4	54.4	9.8	1.54	113	11.8

The open porosity was measured for test specimens with an Archimedes method using butyl alcohol, the density by their dimensions and the weight, and the volume fraction by their dimensions and the weight and the density of fiber.

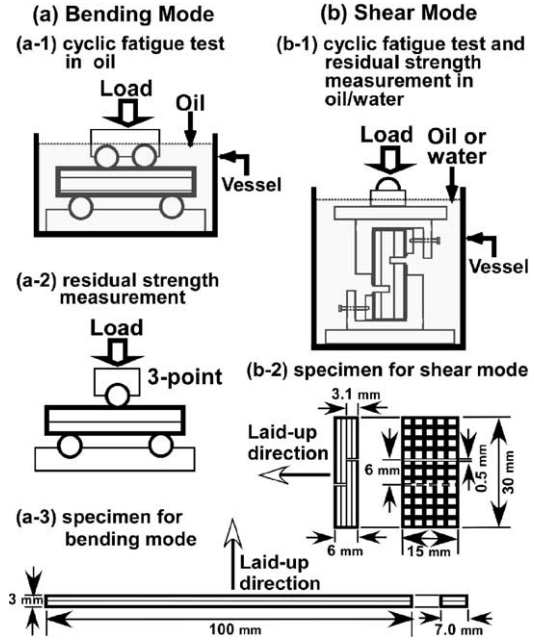

Fig. 1. The specimen's geometry and the test configuration for (a) bending mode and (b) shear mode. In doing tests/measurements in air, they were carried out without the vessel containing water/oil.

pitch-impregnated matrix (Pi3 indicates three times pitch impregnation), by pressing (no-"V" in the notation) and vacuum ("V" in it), respectively, whose properties are compiled in Table 1. This fabric had ca. 4.4 tows in one centimeter for each direction and ca. three layers in one millimeter along the laid-up direction. They were machined into rectangular shapes, 3-mm thick in the laid-up direction and in 7-mm width and 100-mm length. The specimen's geometry is schematically illustrated in Fig. 1.

2.1.2. Static strength

Three-point bending tests were carried out in ambient air with an 80-mm span and a crosshead speed of 0.5 mm/min using five specimens for each. Residual strength after cyclic fatigue tests was also measured with the same method using three specimens for each. Residual strength after cyclic fatigue tests in oil was also measured in oil without any exposure of the samples to air. The calculation of the strength in the bending mode was carried out at the maximum stress. The loading edges had a diameter of 5 mm. The test configuration is schematically illustrated in Fig. 1.

2.1.3. Cyclic fatigue tests

Cyclic fatigue tests were carried out in a four-point bending mode with 14-mm inner-span and 52-mm outer-span using a piezo-bimorph-type fatigue-test machine (NGK Spark Plug Co., Ltd., CFT-340-1M). The maximum applied stress (σ_{max}) was 80% of the average static bending strength of the specimens in ambient air, and a stress ratio (R: ratio of minimum stress to maximum stress) of 0.7, 0.8 or 0.9 was adopted for 10^6 or 10^7 cycles at a frequency of ca. 210 Hz. Specimens for the fatigue tests in oil were evacuated at 10^{-2} Torr for 12 h at 200 °C and soaked in vacuum oil (SunvacOil No.160) without any exposure of them to air. For all the cases, the diameter of the loading edges was 5 mm. The schematic illustration for the test is shown in Fig. 1.

2.2. Fatigue in the shear mode

2.2.1. Materials

Six types of laid-up C/C composites reinforced with woven fabrics, C6-Pi1, C6-Pi3, C6-Pi3-V, CN6-Pi3, C6-Ph3 and CN6-Ph3, and four types of spun-yarn C/C composites, SY-Pi1, SY-Pi4, SY-Ph1 and SY-Ph4, were used in this test mode. All were reinforced with two-dimensional plain-woven fabric and heat treated at 2000 °C. Their properties are also compiled in Table 1. Here, Ph indicates phenol–precursor impregnation by pressing, and N between C and 6 in the notation indicates the as-received surface treatment on the fabric (fiber) was removed by heat treatment at 2000 °C in an inert atmosphere before skeleton preparation, or first impregnation: which implies that CN6 had no/few

oxygen-functional groups on the fabric (fiber). The rule in the notation is same as that in Section 2.1.1(a). No clear mechanical data were available for the spun-yarn fiber, but it had a density of 1.8 g/cm^3 measured using He gas, and the fabric had ca. 5 tows in 1 cm for a direction and ca. four layers in 1 mm along the laid-up direction. Specimens for double-notch compression tests (DNC tests: JIS R-1643) were rectangular with 6-mm thick in the laid-up direction and 15-mm width and 30-mm length, having two notches of 0.5-mm thick and 3.1-mm length at a 6-mm distance. The specimen's geometry is schematically illustrated in Fig. 1.

2.2.2. Static strength

DNC tests were carried out with a crosshead speed of 0.5 mm/min in ambient air, oil or distilled ion-exchanged water (hereafter the word of "water" is used as the de-ionized water) using three to five specimens for each. Residual strength after fatigue testing in oil or water was measured in oil or water without any exposure of the samples to air. The test configuration is illustrated in Fig. 1.

2.2.3. Cyclic fatigue tests

Cyclic fatigue tests were carried out in air, oil or water using specimens set in the same jig for static shear strength measurements by the fatigue test machine. The maximum applied stress was 70%, 80% or 90% of the average static shear strength of the specimens in ambient air with a stress ratio (R) of 0.5 or 0.7, fatigue cycled up to 10^7 at a frequency of ca. 210 Hz. The fatigue tests in oil were done using specimens evacuated at 10^{-2} Torr for 12 h at 200 °C, without any exposure to air. Tested specimens were three for each. The test configuration is shown in Fig. 1.

2.2.4. Static-fatigue tests

The time to break was measured in ambient air using specimens continuously stressed at 90% of the static shear strength in ambient air. The same apparatus for the above tests in Sections 2.2.2–2.2.3 was used for these tests.

3. Results and discussion

3.1. Bending

Specimens did not break in all the fatigue tests. Therefore, residual strength was measured after the fatigue tests, and is shown in Fig. 2. The static strength is also depicted in the figure. The stress–strain curves of all the specimens seemed to be linear, excepting their final stage. No plateaus and drops were observed before reaching the maximum stress, and in most cases a significant drop was observed just after the maximum. The

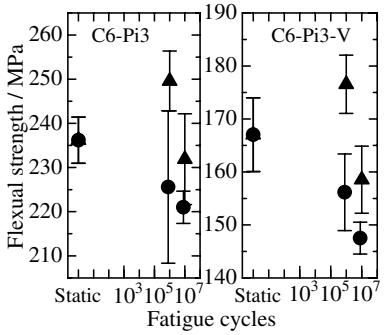

Fig. 2. Residual flexural strength after cyclic fatigue tests in air as a function of fatigue cycles for C6-Pi3 and C6-Pi3-V. The signs show averaged values and the bars the standard deviation. Maximum applied stress in the fatigue tests was 80% of the static strength in air. Closed circles indicate $R = 0.9$ and closed triangles $R = 0.8$.

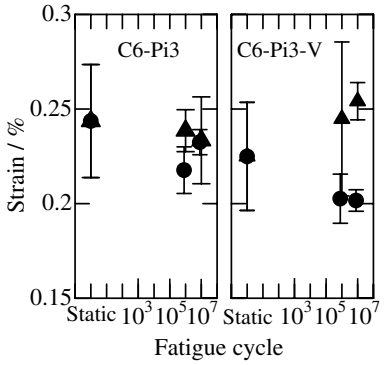

Fig. 3. Strain to the initial drop in stress after cyclic fatigue tests in air as a function of fatigue cycles for C6-Pi3 and C6-Pi3-V. The signs show averaged values and the bars the standard deviation. Maximum applied stress in the fatigue tests was 80% of the static strength in air. Closed circles indicate $R = 0.9$ and closed triangles $R = 0.8$.

strains at the drops are compiled in Fig. 3. For C6-Pi3, no clear significant difference could be seen after fatigue tests as compared with the pristine C6-Pi3. However, a slight increase was measured at $R = 0.8$, while a slight decrease at $R = 0.9$ for C6-Pi3-V after fatigue tests. A crack initiated at the tensile-mode side for all specimens, which was provided by observing a usual speed video recording. Then, the strength was calculated at the maximum load, and the modulus was estimated from the linear portion, between 15 and 115 MPa in stress. The residual strength of both C6-Pi3 and C6-Pi3-V increased for 10^6 cycles at $R = 0.8$, but decreased at $R = 0.9$ with the cycles. The residual strength of both specimens seemed to decrease for 10^7 cycles.

Fig. 4 shows the Young's modulus calculated from the stress–strain diagrams in the measurements of the residual strength at an early linear portion of the diagram. The modulus of un-fatigued/pristine specimens is also shown in the figure. It decreased with increasing the cycles. A threshold in the number of cycles seemed to exist and the threshold increased with decreasing the

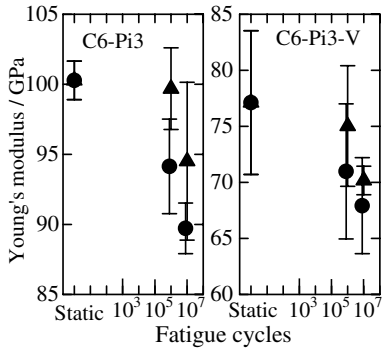

Fig. 4. Young's modulus after cyclic fatigue tests in air as a function of fatigue cycles for C6-Pi3 and C6-Pi3-V. The signs show averaged values and the bars the standard deviation. Maximum applied stress in the fatigue tests was 80% of the static strength in air. Closed circles indicate $R = 0.9$ and closed triangles $R = 0.8$.

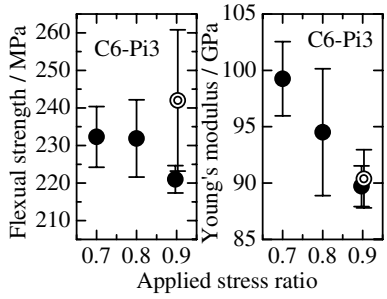

Fig. 5. Residual flexural strength and Young's modulus of C6-Pi3 after cyclic fatigue tests of 10^7 cycles as a function of applied stress ratios. The signs show averaged values and the bars the standard deviation. Maximum applied stress in the fatigue tests was 80% of the static strength in air. Closed circles indicate fatigue tested in air and double circles in oil.

stress ratio. These facts indicate that fatigue of C/C composites in bending was affected by a product/integral of time and stress, not by the number of fatigue cycles as in usual ceramic materials [14].

Fig. 5 shows the modulus and residual strength as a function of the stress ratios for C6-Pi3 fatigue cycled at 10^7 cycles. The ratio of 0.9 resulted in decreasing the strength, and the modulus decreased with the ratio in air. The strength, on the contrary, did not decrease in the case of the fatigue test in oil. However, the modulus fatigue tested in oil decreased with the ratio as was observed in air. Since static strength and modulus in oil were similar to those in air, the measured difference might be caused by cyclic fatigue tests. Micro-cracking affecting the modulus was initiated during fatigue tests in oil as was in air. However, crack propagation affecting the strength did not occur during the fatigue tests in oil even at a high R, which strongly implies that stress corrosion by water vapor may take place in air and that micro-cracks expanded to become larger cracks.

3.2. Shear

Table 2 shows residual strength after cyclic fatigue tests and static shear strength for various specimens. A decrease in strength after cyclic fatigue tests was observed in air for SY-Pi4 and SY-Ph1. For C6-Pi3, static strength in water was lower than that in air. In these three, all specimens were fractured/broken before 10^7 cycles fatigue tested in water. Other specimens, which did not show a clear decrease in strength after cyclic fatigue tests in air, showed no clear decease in strength after cyclic fatigue tests both in air and in water; their

Table 2
Static shear strength and residual strength of the C/C composites

Specimen	Shear strength [average (standard deviation)] MPa		Residual shear strength[a] [average (standard deviation)] MPa	
	In air	In water	In air	In water
C6-Pi1	5.76 (0.83)	[b]	5.91 (0.37)	[b]
C6-Pi3	9.78 (0.77)	8.97 (0.55)	9.37 (0.63)	7.33×10^6 cycles[c] (1.23×10^6 cycles)
C6-Pi3-V	6.26 (0.87)	[b]	6.58 (0.58)	[b]
CN6-Pi3	7.36 (0.38)	7.39 (0.40)	7.57 (0.26)	7.62 (0.22)
C6-Ph3	8.21 (0.79)	7.93 (0.59)	8.11 (0.90)	7.97 (0.47)
CN6-Ph3	6.55 (0.39)	6.27 (0.35)	6.75 (0.17)	6.37 (0.19)
SY-Pi1	4.11 (0.12)	4.05 (0.06)	4.10 (0.06) 4.12[d] (0.11)	4.09[d] (0.04)
SY-Pi4	12.69 (0.13)	10.74 (0.20)	11.51 (0.22)	7.50×10^6 cycles[e] (1.51×10^6 cycles)
SY-Ph1	7.06 (0.14)	6.47 (0.11)	4.68×10^6 cycles[c] (2.39×10^6 cycles)	3.82×10^6 cycles[e] (2.37×10^6 cycles)
SY-Ph4	11.79 (0.54)	11.44 (0.16)	11.90 (0.41)	11.45[d] (0.18)

[a] Fatigue tests were carried out at $\sigma_{max} = 80\%$ of the averaged shear strength in air for 10^7 cycles for $R = 0.5$.
[b] Not tested.
[c] Broken at the cycles.
[d] At $\sigma_{max} = 90\%$ of the averaged shear strength.
[e] Broken at the cycles at $\sigma_{max} = 70\%$ of the average shear strength.

residual strength was equal to the static strength of the pristine ones. In this study, no clear effects of interfacial treatments were realized for the fatigue phenomena.

Detailed investigation was carried out using the spun-yarn C/C composites, which showed clear differences in the fatigue tests. The number of cycles to fracture during the cyclic fatigue tests are shown in Fig. 6 for SY-Pi4 and SY-Ph1 with $R = 0.7$ and 0.5. The number increased with increasing R in both specimens.

In Fig. 7, fatigue life, time to fracture in static–fatigue tests, are shown for SY-Pi4 and SY-Ph1 with those in the cyclic fatigue tests. Considering the R in static fatigue tests is one ($R = 1$), the fatigue life increased with R. This fact reveals that fatigue life is strongly affected by the difference in deflection between at the maximum stress and at the minimum stress, not by stress-exposure time above a certain level. In the composites that showed fatigue behavior, debris, which means tiny particles, was observed, even though the amount was very small. Face-to-face scratching between crack faces in a crack may produce the debris during fatigue tests,

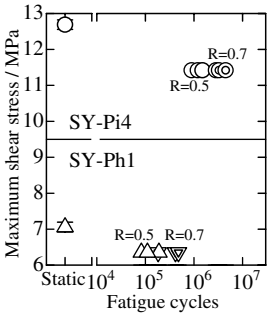

Fig. 6. Static shear strength and fatigued strength in cyclic fatigue tests in air at two different R values ($R = 0.7$ and 0.5) for SY-Pi4 and SY-Ph1. Maximum applied shear stress in the fatigue tests was 90% of the static strength in air. Double circles and double inverse triangles indicate $R = 0.7$, and open circles and triangles $R = 0.5$. The standard deviation in static shear strength, shown by a bar, was smaller than the size of the symbol.

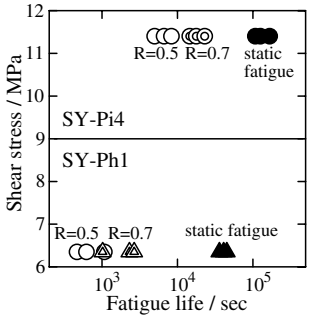

Fig. 7. Fatigue life in air under various conditions for SY-Pi4 and SY-Ph1. Maximum applied shear stress in the fatigue tests was 90% of the static strength in air. Double circles and double triangles indicate cyclic-fatigue tests with $R = 0.7$, open circles and triangles for those with $R = 0.5$, and closed ones for static–fatigue tests.

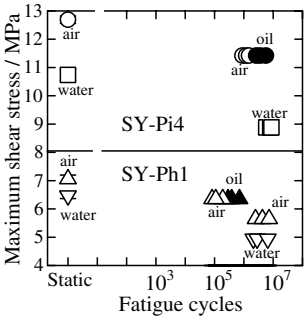

Fig. 8. Static shear strength and fatigued strength in cyclic fatigue tests with $R = 0.5$ under various conditions (in water, air or oil) for SY-Pi4 and SY-Ph1. The standard deviation in static shear strength, shown by a bar, was smaller than the size of the symbol.

because the crack faces were not flat; weaving reinforcements, domain structures of the impregnated matrix, etc., played a role. The debris prevented closing the crack to the original position, resulting in a mismatch of crack faces, and further enhanced the actual stress at the tip of the crack. This was similar to the mechanism caused by a wedge effect [15,16] in ceramics. A smaller R provides larger variation in crack-opening distance during a fatigue test, resulting in a larger mismatch and severe fatigue of the specimen.

The above fact in the shear mode was much different from that in the bending one, in which decreases in strength increased with R. It is implied that the wedge effect strongly affects crack propagation in the shear mode, but not so much in the bending one, which may originate because the strength in the former mode is dominated by matrix but by reinforcements/fibers in the latter. In bending modes, it might also be considered that a stress that caused a decrease in crack-opening distance in the specimens affected the wedge effect.

Degradation in strength was accelerated in water than in air, i.e., in water specimens were fractured at a small number of cycles or a decrease in strength was caused by lower stress as compared in air as shown in Fig. 8. In oil, the degradation was retarded.

The above-mentioned results strongly suggest that fatigue degradation of C/C composites seems to progress by a combination of a wedge effect [15,16] changing stress levels at the crack–tip [17] and a type of stress corrosion with water [14].

4. Summary

Fatigue tests in the bending and shear modes were carried out using several kinds of C/C composites. The following conclusions were reached: Fatigue degradation could occur in both modes between 10^4 and 10^7 fatigue cycles. Degradation in fatigue increased with stress ratio in bending, but decreased in shear. For specimens showing fatigue degradation in air, water

strongly affected not only fatigue degradation but also the static strength in water; i.e., the strength in water was lower than that in air. It is strongly suggested that fatigue of C/C composites proceeds by a combination of a wedge effect and stress corrosion with water.

Acknowledgements

This study was partly supported by a grant-in-aid for scientific research (B) of JSPS. The authors acknowledge Prof. T. Akatsu of Materials and Structures Laboratory, Tokyo Institute of Technology for his helpful discussions.

References

[1] Roy AK. Tensile fatigue behavior of a coated two-dimensional carbon–carbon composite laminate. J Compos Technol Res 1996;18:202–8.
[2] Mostafa I, Moet A. Effect of processing flaws on the fracture toughness of two-dimensional carbon–carbon composite. J Mater Sci Lett 1996;15:755–8.
[3] Christel PM, Meunier A, Leclercq S, Bouquet P, Buttazzoni B. Development of a carbon–carbon hip prosthesis. J Biommed Mater Res 1987;21:191–218.
[4] Ozturk A, Moore RE. Tensile fatigue behaviour of tightly woven carbon/carbon composites. Composites 1992;23:39–46.
[5] Mahfuz H, Maniruzzaman M, Krishnagopalan J, Hague A, Ismail M, Jeelani S. Effects of stress ratio on fatigue life of carbon–carbon composites. Theor Appl Fract Mech 1995;24:21–31.
[6] Ozturk A. The influence of cyclic fatigue damage on the fracture toughness of carbon–carbon composites. J Biomed Mater Res 1996;27A:641–6.
[7] Williams JC, Yurgartis SW, Moosbrugger JC. Interlaminar shear fatigue damage evolution of 2-D carbon–carbon composites. J Comp Mater 1996;30(7):785–99.
[8] Fend T, Goering J. Strength and fatigue behavior of 2D-carbon/carbon composites under shear conditions. Ceram Trans 1994;46:165–76.
[9] Goto K, Hatta H, Katsu D, Machida T. Tensile fatigue of a laminated carbon-carbon composite at room temperature. Carbon 2003;41:1249–55.
[10] Sogabe T, Yoda S, Ioku I, Araki T, Oku T. Mechanism of delayed fracture of polycrystalline graphite. J Soc Mater Sci Jpn 1985;34:1437–40 [in Japanese].
[11] Kobayashi H, Arai Y, Nakamura H, Araki T, Oku T. Evaluation of fracture mechanics characteristics of a high strength graphite IG-11. J Soc Mater Sci Jpn 1988;37:934–8 [in Japanese].
[12] Maruyama T, Nishimura Y. Effect of adsorbed gases on mechanical properties of nuclear graphite. TANSO 1992(152);1992:98–105 [in Japanese].
[13] JUTEM (Japan ultra-high temperature material research center), A NEDO report on durability of super heat-resistant composites under ultra-high temperatures. NEDO, 1994:35–7 [in Japanese].
[14] Ritchie RO, Dauskardt RH. Cyclic fatigue of ceramics. J Ceram Soc Jpn 1991;99:1047–62.
[15] Okazaki M, McEvily AJ, Tanaka T. On the mechanism of fatigue crack growth in silicon nitride. Metall Trans 1991;22A:1425–6.
[16] Kawakubo T, Goto A. Cyclic fatigue behavior of ceramics at room temperature. J Soc Mater Sci Jpn 1987;36:1253–8 [in Japanese].
[17] Ueno A, Kishimoto H, Ookawara S, Kondo T, Yamamoto A. Crack propagation behavior of small crack of polycrystalline alumina and effects of cyclic load and grain size on bridging. J Soc Mater Sci Jpn 1994;43:183–9 [in Japanese].